

# MIMO Indoor WLAN Channel Measurements and Parameter Modeling at 5.25 GHz

Aditya K. Jagannatham  
UC SanDiego  
9500 Gilman Drive  
La Jolla, CA-92093  
e-mail: ajaganna@ucsd.edu

Vinko Erceg  
Zyray Wireless  
11455 El Camino Real  
San Diego, CA-92130  
verceg@zyraywireless.com

**Abstract**— We present measurement results of indoor multiple-input multiple-output (MIMO) multipath wireless channels in the Unlicensed National Information Infrastructure (U-NII) 5.25 GHz band for wireless local area network (WLAN) applications. MIMO channel impulse responses were measured at different locations using co-polarized (copol) and cross-polarized (crosspol) antennas under line-of-sight (LOS) and non-line-of-sight (NLOS) channel conditions in office and cafeteria type environments. Ricean K-Factors, correlations, crosspol discriminations (XPD), pathloss ( $PL$ ) and RMS delay spread ( $\tau_{rms}$ ) were computed for different antenna configurations (copol/crosspol) and different channel conditions (LOS/NLOS). Models were developed to characterize the distance dependent variation and the statistical deviations of these parameters.

## I. INTRODUCTION

MIMO systems have gained considerable attention recently for possible deployment in current and forthcoming wireless systems. Among the many gains that MIMO systems offer, the most interesting is the capacity of these systems which increases linearly with the number of antennas [1]. Another attractive feature of such systems is the diversity advantage they offer which can be used to combat the significant problems of fading and multi-user interference in wireless channels. Such benefits make it a coveted technology to solve the increasing bandwidth needs in systems requiring high data rates such as wireless local area networks (WLANs), wireless broadband access (WBA), and third and fourth generation wireless systems (3G and 4G).

Most studies related to the achievable performance of MIMO systems consider simplistic channel models. These models have limited utility for practical studies which necessitate realistic channel models. More accurate channel models would require in depth analysis and statistical characterization of actual data collected over MIMO wireless systems. The associated K-factors, crosspol discriminations (XPD), antenna correlation and pathloss have a high bearing on the wireless channel capacity. For example, the channel capacity is especially very sensitive to the K-factor which influences the rank properties of the channel matrix. Hence, these quantities and their effects need to be modeled accurately to generate models that closely resemble the true wireless channel.

Models for MIMO communication channels which discuss specific modeling and performance aspects such as time and

angle of arrival [2], [3], [4], correlation properties [5], [6], polarization diversity [7], [8], [9] can be found in existing literature. However, a unified study of a MIMO channel that encompasses different parameters and especially a multipath channel has rarely been reported. An integrated channel model that includes parameters such as pathloss, K-factor, XPD and antenna correlation was presented in [10], [11] for the fixed wireless outdoor flat fading  $2 \times 2$  MIMO channel at 2.4 GHz. However, indoor channels tend to have significantly different characteristics when compared to outdoor channels. A tutorial survey on the subject of indoor single-input single-output (SISO) channel models and comparison with outdoor channel models can be found in [12], [13]. Our channel modeling study aims to provide simulation models for the indoor MIMO channel in the 5.25 GHz U-NII band.

In this paper we present  $4 \times 4$  and  $3 \times 3$  MIMO channel measurement results in the 5.25 GHz unlicensed band for indoor WLAN applications. The measured data was used to compute the distance dependent K-factor, antenna correlation, and XPD properties. Similar modeling strategy was used in [11] to model the outdoor fixed wireless channel in the 2.4-2.5 GHz band. These models were then used to simulate multipath MIMO channels in [14] and the calculated capacities of the model were found to be in close agreement to that of the actual data. Also in the same work, benefits of this accurate model over the simplistic iid realizations are shown.

## II. MEASUREMENT SETUP

MIMO channel measurements were carried out in the 5.25 GHz band over  $4 \times 4$  and  $3 \times 3$  MIMO channels. The commercially available measurement equipment (Elektrobit) used for this purpose employed a direct-sequence spread-spectrum sliding correlator to resolve the arriving multipath signals. Data was collected at 30 different locations in two different environments. The first was a typical office environment which has a long corridor with offices alongside and hence offers a more hostile blockade to the wireless signal. The second is a typical cafeteria (hotspot) environment which is relatively more open. The time resolution of the channel impulse responses (delay between successive paths) was 10 ns. A total of 100 paths were measured for each channel instantiation. The maximum delay of each impulse response

was  $1\mu s$ . Each measurement was made over a distance of 2.5 m and data was collected for a total of 500 multipath MIMO channel snapshots (i.e.  $5 \times 10^4$  complex MIMO channel matrices) for a duration of 10 s at each distance. Therefore, 50 multipath MIMO channels were measured every second. The experiment was repeated twice at each distance to obtain better statistical averaging. The transmit and receive antennas were at a height of 1.2 m above the floor.

Standard dipole type antennas were used to carry out the experiments. Antenna arrays of different configurations and spacings were employed. The first was an all vertical (copol) antenna configuration which employed 4 antennas arranged in a horizontal square with  $\lambda/2$  separation along the sides of the square. The second was a cross-polarized (crosspol) antenna configuration which employed 3 co-located antennas both at the transmit and receive side. These 3 antennas were at right angles with respect to each other, one vertical and two in the horizontal plane. The different configurations mentioned above exhibit significantly different received signal characteristics and hence have been modeled separately. The recorded data was streamed to a computer for later processing.

### III. MODELING DIFFERENT PARAMETERS

From the data collected, paths with two different characteristics have been observed from every multipath MIMO channel realization. The first is a single **strong** path with the highest concentration of signal power due to the strong signal component along the line joining the transmitter and receiver, usually the LOS path. The rest of the paths with relatively less signal power arise primarily because of reflections from adjacent scatterers and hence are termed as **scatter** paths. Every multipath profile instantiation consists of one strong LOS path and many scatter paths. Hence each multipath MIMO channel matrix  $\mathbf{H}(t)$  can be modeled as

$$\mathbf{H}(t) = \sqrt{P_s}H(0)\delta(t) + \sum_{k=1}^{N_p} \sqrt{\frac{P_s}{\xi}} e^{-kt_p/2\tau_{rms}} H(k)\delta(t-kt_p), \quad (1)$$

where  $H(0)$  is the channel matrix associated with the strong path, and  $H(k)$  with  $k \geq 1$  are the channel matrices associated with scatter paths,  $\tau_{rms}$  is the RMS delay spread,  $P_s$  is the received power of the strong path and the quantity  $\xi$  is the excess power in the strong path above the profile (explained in Sec. III-A). The K-factor, correlation and XPD values of the strong path (channel matrix  $H(0)$ ) exhibit significantly different characteristics as compared to those of the scatter paths (channel matrices  $H(k)$ ,  $k \geq 1$ ). Hence in our modeling we choose to model the parameters corresponding to the two different path types separately.

The strong path parameters of a multipath MIMO channel can be seen to exhibit a variation which can be resolved as a sum of two effects. The first is a large scale variation with distance arising primarily because of the increase in the number of scatterers and a decrease in the signal power due to the transmitter and receiver separation distance. This variation of the parameter is well modeled by a distance dependent

mean (DDM). The second effect arises from the randomness inherent in the surrounding scattering environment and its effect can be manifested as a fluctuation of the parameter value around the mean for a given distance. This net variation of a parameter can be modeled as resulting from the sum of a DDM and a stochastic quantity  $X_{rand}$  having a certain variance  $\sigma$ . The specific modeling technique of each parameter type then follows the one detailed in [11]. For each parameter we compute the distance dependent mean (DDM) by a linear regression of the its value versus log distance (for log-normal parameters such as K-factor, XPD,  $P$  and  $\tau_{rms}$ ) or versus linear distance (for linear parameters such as receive and transmit correlation). We then compute the variance of their deviations about the DDM. Thus the variation of a given log-normal parameter is modeled as

$$\theta_n(dB) = m_n \log_{10} d + X_0 + \sigma_n X_{rand}, \quad (2)$$

where  $m_n$  and  $X_0$  indicate the slope in dB/decade and intercept value in dB, respectively.  $\sigma_n$  represents the variance of the deviation of the parameter over its DDM and  $X_{rand}$  is a zero-mean unit-variance random variable (the Gaussian nature of which will be shown in later sections). Analogously, a linear parameter is modeled as

$$\theta_l = m_l d + X_0 + \sigma_l X_{rand}, \quad (3)$$

where  $m_l$  is the slope of the line,  $X_0$  is the intercept, and  $\sigma_l$  and  $X_{rand}$  are analogously defined as in the log-normal case above. In later sections, we model the deviations over the DDM in greater detail to replicate accurately the statistical nature of the parameters. The parameters associated with scatter paths were found to exhibit only a weak dependence on distance and hence are modeled as a random fluctuation over a constant mean (i.e.  $m = 0$ ).

Further, to compute the above parameters we use the signal power rather than the complex channel coefficients to avoid the problems arising from a slow phase drift inherent in the measurement system. However, the measurements have been accurate enough to preserve the relative phases between different elements of each MIMO channel matrix.

#### A. Delay Profile

A typical delay profile is given in Fig. 1. The strongest path exhibits an impulsive power component above the multipath profile. Such profiles can be accurately modeled using the 'spike + exponential' model detailed in [15]. The impulsive power component ( $\xi$ ) of the spike was computed and averaged over distance and different antenna configurations to yield  $\xi_{LOS} = 6.83$  dB and  $\xi_{NLOS} = 2.32$  dB. This is similar to the value of 7 dB reported in [15] for outdoor LOS channels. As expected,  $\xi_{NLOS}$  was found to be lower than  $\xi_{LOS}$ .

#### B. K-factor

We have computed K-factor via the moment-method technique detailed in [16]. The K-factor for each  $R_x - T_x$  pair of each path tap was computed using the 500 channel instantiations. As mentioned above in Sec. III, the K-factors

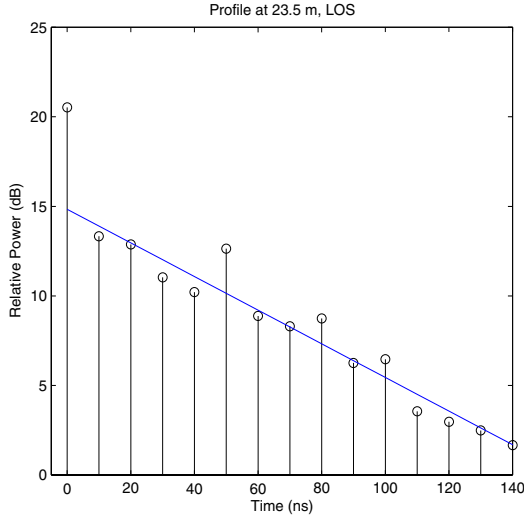


Fig. 1. Delay Profile, LOS at 23.5 m.

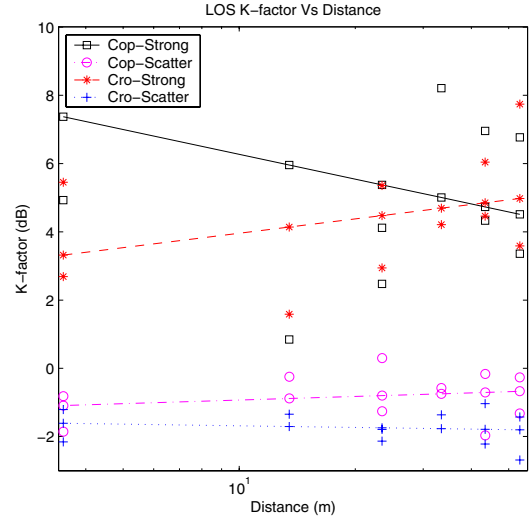


Fig. 2. Copol and Crosspol K-factor, LOS, Strong Path (Strong = strong path, Scatter = scatter path, Cop = Copol, Cro = crosspol).

of the strong and scatter paths exhibit different statistical characteristics. Thus the K-factors of each strong path were averaged over different antenna pairs while the K-factors of the scatter paths were averaged over the different scatter paths and antenna pairs.

Plot of K-factor in dB (including LMSE fit) vs. distance for LOS condition is shown in Fig. 2. The LOS K-factor for the strongest path is found to be significantly higher (6 - 7 dB) than that of the scatter paths. The copol K-factor was higher than the crosspol K-factor by 3 dB, a trend reported in [9]. The DDMs of these coefficients are given in the Table I and Table II.

### C. Antenna Correlation

Correlation studies of MIMO channels have been made previously in [5],[6]. In our analysis we have computed the complex envelope correlation coefficient given in [16] which represents the worst-case (upper bound) correlation between signal paths. The correlation coefficients for all possible receive and transmit combinations (24 for a  $4 \times 4$  copol MIMO matrix and 18 for the  $3 \times 3$  crosspol MIMO matrix) were computed for each tap (by using the 500 channel instantiations). The  $R_x$  and  $T_x$  correlation coefficients of the strong and scatter paths were then averaged separately at each distance to compute the mean  $R_x$  and  $T_x$  correlation coefficient for that location. The DDM and  $\sigma$  parameters were then obtained by the same technique used for the K-factor detailed in Sec. III-B.

The scatter plots of correlation coefficient vs. distance for different path types are given in Fig. 3. For the LOS conditions, correlation was found to increase with distance. This is explained by the decrease in the angular spread seen at the receiver and transmitter over the narrow indoor corridors with distance. A similar trend was observed in [6] where correlation properties of indoor MIMO channels were studied. At ranges of 30 m - 50 m (100 ft - 150 ft) the correlation was

found to increase from around 0.5 to 0.7 which is consistent with our analysis. Moreover, the transmit correlation is slightly higher than the receive correlation, a trend confirmed by [6]. As expected, the correlation coefficients for the strong paths were found to be significantly higher than those for the weaker scatter paths. For the copol case, since the transmit and receive correlation values are close to each other, we report an average value for the antenna correlation. Further, the crosspol correlation coefficients were found to be close to 0 due to the additional polarization dimension in the crosspol case (where signals experience significant scattering, i.e. decorrelation).

### D. Cross-Polarization Discrimination (XPD)

We computed the fixed and variable signal component XPDs ( $XPD_c$  and  $XPD_v$ , respectively), similar to the approach in [10], [11]. For each  $T_x - R_x$  antenna pair, the constant and variable pathpower was computed using the technique detailed to calculate the K-factor in Sec. III-B above and employing the data points across 500 instantiations. The XPD values per path were then computed as the ratio of the mean power of the 3 co-polarized antenna pairs ( $T_x^1 - R_x^1$ , etc.) to the mean power of the 6 cross-polarized antenna pairs ( $T_x^1 - R_x^2, T_x^2 - R_x^1$ , etc.) for each path. The XPD for each path type was then averaged separately to compute the value of XPD at a given location.

The plot of XPD vs. distance is shown in Fig. 4. It can be observed that the NLOS XPDs are significantly lower than their LOS counterparts due to the presence of significant scattering (depolarization) for the NLOS conditions. Also, the presence of a dominant direct component in the strong path results in a higher XPD for it compared to the scatter paths. In most cases the XPDs can be observed to be independent with distance except for the decreasing trend of the constant signal XPD of the strong path. It can also be verified that

$$K_{copol}(dB) \approx K_{crosspol} + XPD_c - XPD_v, \quad (4)$$

as shown in [11]. For example, at a distance of 10 m for the strong path,  $K_{copol} = 8.69 \text{ dB} - 2.41 \text{ dB} = 6.28 \text{ dB}$ . Similarly,  $K_{crosspol} = 2.56 \text{ dB} + 1.40 \text{ dB} = 3.96 \text{ dB}$ . Also,  $XPD_c = 8.40 \text{ dB}$ , and  $XPD_v = 6.78 \text{ dB}$ . It can now be seen that  $K_{copol} - K_{crosspol} = 2.32 \text{ dB} \approx 1.62 \text{ dB} = XPD_c - XPD_v$ .

### E. RMS Delay Spread

The RMS delay spread ( $\tau_{rms}$ ) characterizes the spread of the multipath signal energy arising from scattering. This parameter in models the relative amplitude of the different signal arrival paths. A rigorous treatment of RMS delay spread modeling can be found in [17]. The RMS delay spread ( $\tau_{rms}^c$ ) for a continuous path power profile is given theoretically by the relation

$$\tau_{rms}^c = \sqrt{\frac{\int (t - \bar{t})^2 |s(t)|^2}{\int |s(t)|^2}}, \quad \bar{t} = \frac{\int t |s(t)|^2}{\int |s(t)|^2},$$

where  $s(t)$  is the complex channel gain as a function of time  $t$ . In our analysis, at each given location, the MIMO power profiles were averaged over 500 channel instantiations to produce a single multipath MIMO profile. The RMS delay spread for each  $T_x - R_x$  antenna combination was then computed as

$$\tau_{rms}^{i,j} = \sqrt{\frac{\sum_{p=1}^{N_p} (pt_d - \bar{t})^2 |h_{ij}^p|^2}{\sum_{p=1}^{N_p} |h_{ij}^p|^2}}, \quad \bar{t} = \frac{\sum_{p=1}^{N_p} pt_d |h_{ij}^p|^2}{\sum_{p=1}^{N_p} |h_{ij}^p|^2}.$$

$N_p$  denotes the total number of paths in the multipath MIMO profile ( $N_p = 100$  in our analysis),  $h_{ij}$  denotes the complex channel coefficient between the  $i$ -th receiver and  $j$ -th transmitter,  $p$  represents the path index and the constant  $t_d$  denotes the time delay between successive arrival paths (10 ns). The delay spread was then averaged over all antenna combinations to give the average delay spread ( $\tau_{rms}$ ) at a given location.  $\tau_{rms}$  was found to increase with distance from 25 to 50 ns as observed in [18].

### F. Received Signal Power

At each location, the received signal power of the strong path for each antenna combination was computed. The strong path received power was then averaged over the 500 instantiations and all antenna combinations to yield the value of the average received strong path power ( $P_s$ ) for a given distance. The same scheme was followed in the crosspol case, except that only the co-aligned antenna combinations ( $R_x^k - T_x^k$ ,  $k = 1, 2, 3$ ) were used. The received signal power for cross-polarized antenna combinations can be computed by further attenuating the signal power for co-aligned antennas by the XPD thus making the modeling consistent. The total received signal power ( $P$ ) can be obtained from the strongest path power  $P_s$  as

$$P = P_s + P_s \xi^{-1} \sum_{k=1}^{N_p} e^{-kt_p/\tau_{rms}}. \quad (5)$$

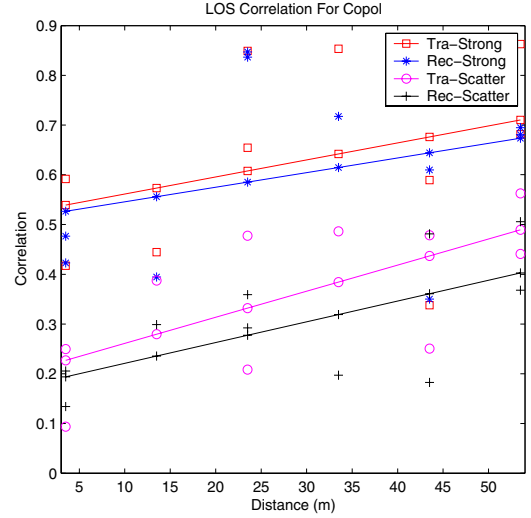


Fig. 3. Transmit and Receive Correlation, LOS (Tra = transmit, Rec = receive).

Par	LOS			NLOS		
	m	$X_0$	$\sigma$	m	$X_0$	$\sigma$
$PL_s$	20.70	46.66	2.60	36.74	44.48	5.07
$\tau_{rms}$	2.52	12.94	1.01	2.04	11.90	1.44
K-St	-2.41	8.69	3.25	-2.30	2.68	1.07
Co-St	0.0032	0.52	0.18	-0.0027	0.52	0.25
K-Sc		-0.79	0.74		-2.34	0.41
Co-Sc		0.31	0.11		0.22	0.11

TABLE I

DDM PARAMETERS OF COPOL ANTENNAS (PAR = PARAMETER, K = K-FACTOR, Co = CORRELATION, St = STRONG, Sc = SCATTER). ALL PARAMETERS ARE IN dB EXCEPT CORRELATION WHICH IS LINEAR.

The pathloss of the strong path  $PL_s$  is higher for NLOS conditions, as expected, because of the absence of a direct strong LOS component. The LOS slope of approximately 20-25 dB/decade agrees with the range of the pathloss exponent  $n$  reported in [12] for indoor wireless channels and specifically office type environments.

## IV. MODELING VARIATION ABOUT DDM

To model the wireless channel parameters at each location, it is necessary to accurately model the random fluctuation of each parameter about its corresponding DDM. It was observed that the parameters K-factor, XPD,  $\tau_{rms}$  and pathloss exhibit a log-normal deviation over the DDM. Similar trends were observed in outdoor channels [17],[19]. Antenna correlation was found to have a Gaussian deviation. Also, the correlation between the deviations of different quantities was found to be close to 0. Thus, these deviations can be generated using iid Gaussian random variables. From the deviations and the DDM relations given in Table I and Table II, a scheme has been proposed in [14] for MIMO channel model construction.

Par	LOS			NLOS		
	m	$X_0$	$\sigma$	m	$X_0$	$\sigma$
$PL_s$	20.70	46.66	2.60	36.74	44.48	5.07
$\tau_{rms}$	2.52	12.94	1.01	2.04	11.90	1.44
K-St	1.40	2.56	1.70	-4.03	3.26	1.55
$X_c$ -St	-2.23	10.63	2.73	-4.75	8.54	1.88
$X_v$ -St	-0.05	6.83	1.65	-3.10	6.16	0.93
K-Sc	-1.74	0.54		-2.80	0.56	
$X_c$ -Sc	6.15	0.69		2.11	1.46	
$X_v$ -Sc	4.29	0.47		1.81	0.63	

TABLE II

DDM PARAMETERS OF CROSSPOL ANTENNAS. (PAR = PARAMETER, K = K-FACTOR,  $X_c$  = CONSTANT SIGNAL XPD,  $X_v$  = VARIABLE SIGNAL XPD, St = STRONG, Sc = SCATTER, CORRELATION = 0). ALL PARAMETERS ARE IN dB EXCEPT CORRELATION WHICH IS LINEAR.

## V. CONCLUSION

In this paper, we present a study of the indoor MIMO wireless channel at 5.25 GHz. The parameters such as K-factor, correlation, XPD, RMS delay spread and pathloss were studied for different channel conditions (LOS or NLOS) and different antenna configurations (copol and crosspol). Simple models were developed for the distance dependent mean and Gaussian deviations about the mean. MIMO channel models simulated utilizing these parameters can thus be employed in practical studies to analyze the end-to-end performance of systems under a variety of indoor channel conditions and antenna configurations.

## VI. ACKNOWLEDGEMENTS

We would like to thank Daniel Baum, Helmut Bölcskei, Casimir Schmid and Peter Müller for their assistance in collection and processing of measurement data. We would also like to thank Pieter van Rooyen for making the measurement campaign possible.

## REFERENCES

- [1] G.J. Foschini and M.J. Gans, "On limits of wireless communications in a fading environment when using multiple antennas," *Wireless Personal Communications*, vol. 6, pp. 311–335, Mar. 1998.
- [2] Q. Spencer, B. Jeffs, M. Jensen, and A. Swindlehurst, "Modeling the statistical time and angle of arrival characteristics of an indoor environment," *IEEE Journal on Selected Areas in Communications*, vol. 18, no. 3.
- [3] R.J.M. Cramer, R.A. Scholtz, and M.Z. Win, "Evaluation of an ultra-wide-band propagation channel," *IEEE Transactions Antennas and Propagation*, vol. 50, no. 5.
- [4] L. Schumacher, K. I. Pedersen, and P.E. Mogensen, "From antenna spacings to theoretical capacities - guidelines for simulating MIMO systems," *Proc. PIMRC Conf.*, vol. 2, pp. 587–592, 2002.
- [5] J.P. Kermaol, L. Schumacher, P.E. Mogensen, and K.I. Pedersen, "Experimental investigation of correlation properties of MIMO radio channels for indoor picocell scenarios," *Proc. IEEE Vehicular Technology Conf., Boston, USA*, vol. 1, pp. 14–21, 2000.
- [6] P. Kyritsi and D.C. Cox, "Correlation properties of MIMO radio channels for indoor scenarios," *Proc. Signal Systems and Computers 35th Asilomar Conf.*, vol. 2, 2001.
- [7] P. Kyritsi, "Propagation characteristics of horizontally and vertically polarized electric fields in an indoor environment: simple model and results," *Proc. IEEE VTC 2001 Fall*, vol. 3, pp. 1422–1426, 2001.

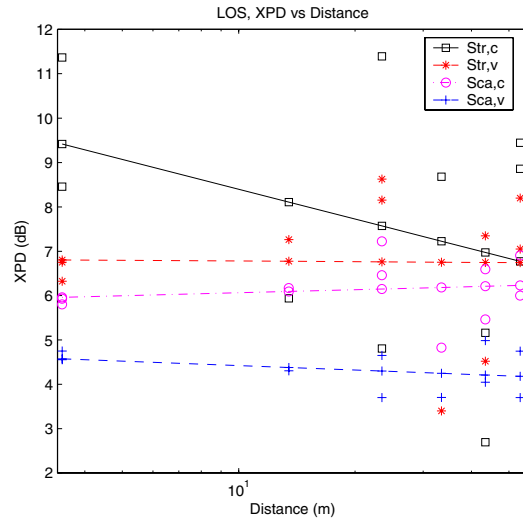


Fig. 4. Constant and variable signal XPD, LOS, Strong Path (Str = strong path, Sca = scatter path, c = constant, v = variable).

- [8] J.P. Kermaol, L. Schumacher, F. Frederiksen, and P.E. Mogensen, "Polarization diversity in MIMO radio channels: experimental validation of a stochastic model and performance assessment," *Proc. IEEE VTC 2001 Fall*, vol. 1, pp. 22–26, 2001.
- [9] S. Loredó, B. Manteca, and R. Torres, "Polarization diversity in indoor scenarios: an experimental study at 1.8 and 2.5 GHz," *Proc. PIMRC*, vol. 2, pp. 896–900, 2002.
- [10] P. Soma, D.S. Baum, V. Erceg, R. Krishnamoorthy, and A.J. Paulraj, "Analysis and modeling of multiple-input multiple-output (MIMO) radio channel based on outdoor measurements conducted at 2.5 GHz for fixed BWA applications," *Proc. IEEE ICC'2002*, Apr. 2002.
- [11] V. Erceg, D. S. Baum, P. Soma, and S. Catreux, "Multiple-input multiple-output fixed wireless radio channel measurements and modeling using dual-polarized antennas at 2.5 GHz," *Accepted for publication in IEEE Trans. on Wireless Communications*, 2004.
- [12] H. Hashemi, "The indoor radio propagation channel," *Proceedings of the IEEE*, vol. 81, no. 7.
- [13] J.B. Andersen, T.S. Rappaport, and S. Yoshida, "Propagation measurements and models for wireless communication channels," *IEEE Communications Mag.*, pp. 42–49, 1995.
- [14] A.K. Jagannatham and V. Erceg, "Multiple-input multiple-output indoor WLAN channel measurements and modelling at 5.25 GHz," *In preparation*.
- [15] V. Erceg et al, "A model for the multipath delay profile of fixed wireless channels," *IEEE Journal on Selected Areas in Communications*, vol. 17, no. 3, pp. 399–410, Mar. 1999.
- [16] D.G. Michelson, V. Erceg, and L.J. Greenstein, "Modeling diversity reception over narrowband fixed wireless channels technologies for wireless applications," *IEEE MTT-S Symposium*, pp. 95–100, 1999.
- [17] L.J. Greenstein, V. Erceg, Y.S. Yeh, and M.V. Clark, "A new path-gain/delay-spread propagation model for digital cellular channels," *IEEE Transactions on Vehicular Technology*, vol. 46, no. 2.
- [18] A.A.M. Saleh and R.A. Valenzuela, "A statistical model for indoor multipath propagation," *IEEE Journal on Selected Areas in Communications*, vol. 5, pp. 128–137, 1987.
- [19] L.J. Greenstein, S.Ghassemzadeh, V.Erceg, and D.G. Michelson, "Ricean K-factors in narrowband fixed wireless channels: Theory, experiments, and statistical models," *WPMC'99 Amsterdam Conference Proceedings*, 1999.